공학박사 학위논문

# A Study on Development of Silicon-Based Anode for Improved Solid-state Li-ion Batteries

# 개선된 고체 리튬 이온 배터리를 위한 실리콘계 음극 개발에 관한 연구

2023 년 8 월

서울대학교 대학원

재료공학부

정 제 준

# A Study on Development of Silicon-Based Anode for Improved Solid-state Li-ion Batteries

# 개선된 고체 리튬 이온 배터리를 위한 실리콘계 음극 개발에 관한 연구

지도교수 선 정 윤

이 논문을 공학박사 학위논문으로 제출함

2023년 6월


서울대학교 대학원

재료공학부

정 제 준


정제준의 박사 학위논문을 인준함

2023년 6월

위 원 장 한 흥 남 (인)

부위원장 선 정 윤 (인)

위 원 최 인 석 (인)

위 원 오 규 환 (인)

위 원 조 종 수 (인)

# Abstract

# A Study on Development of Silicon-Based Anode for Improved Solid-state Li-ion Batteries

JEONG Jejun

Material Science and Engineering

The Graduate School

Seoul National University

The application of lithium-ion (Li-ion) battery technology is expanding beyond the existing mobile IT devices, its applications also include medium and large-sized power devices for electric vehicles (EVs) and energy storage systems in a large market size. The paradigm of the future automobile industry is shifting to eco-friendly EVs owing to the focus on energy saving, strengthened environmental regulations, and depletion of fossil energy. Accordingly, the demand for secondary batteries and performance and safety is rapidly increasing. The development of high-capacity, safe, and long-life secondary batteries along with technology development for commercialization is progressing in parallel with the development of core materials and cell manufacturing technologies. Currently, organic liquid electrolytes for Li-ion

batteries face stability issues such as flammability, leakage, and temperature vulnerability. Recently, all-solid-state Li-ion batteries that do not use liquid electrolytes and their associated fire risk have been gaining considerable attention. The nonflammable solid electrolyte provides high thermal stability and prevents the risk of explosion. When using a liquid electrolyte, a separator is required to prevent direct contact between the positive and negative electrodes, thereby increasing the internal stability of the battery. However, the solid electrolyte itself acts as a separator. Without the need to add a separator, active materials that increase energy density can be added, enabling high-density batteries. Moreover, there is no risk of side reactions caused by temperature changes or leakage resulting from external shocks.

The second chapter presents investigations on the effect of an artificial $Al_2O_3$ coating between the anode and the solid electrolyte. The demand for high-capacity, safe, and long-life secondary batteries as well as the interest in all-solid-state batteries is growing. The cycle performance of the solid-state batteries is limited by interfacial phenomena at the electrolyte–anode interface, which hinders ion diffusion. A multifunctional aluminum oxide (specifically, $Al_2O_3$) coating was created for application on silicon-based (Si-based) anodes in all-solid-state Li-ion batteries. The coating was applied to provide stable artificial solid electrolyte interphase (SEI) layers on Si-based anodes. $Al_2O_3$ layers not only promote the diffusion of $Li^+$ through Li–Al–O, but also, owing to their intrinsically low electronic conductivity, limit electron transmission at the contact between the anode and the electrolyte. Radio frequency sputtering was employed to create a simple and economical $Al_2O_3$ coating. The cycle

properties of Si-based anodes were enhanced by adding a thin amorphous aluminum oxide layer (i.e., $Al_2O_3$ coating). After 100 charge–discharge cycles, the half cell with the $Al_2O_3$ layer delivered a discharge capacity of 502.08 mAh $g^{-1}$ and a capacity retention ratio of 58.86%. Furthermore, at 100 cycles, the sample without the $Al_2O_3$ layer had a discharge capacity of 278.48 mAh $g^{-1}$ and capacity retention of 34.34%. Therefore, the $Al_2O_3$-coated Si-based anodes were cycled successfully in all-solid-state half-cells, producing functional high-performance Li-ion batteries.

Furthermore, the third chapter presents another artificial lithium phosphorus oxynitride (LiPON) coating on Si-based anodes. Researchers have implemented various protective coatings deposited on top of the anode. One of the representative protective coatings is artificial SEI. Besides $Al_2O_3$, LiPON is one of the most prominent coatings. It exhibits a wide stability voltage window, good Li-ions diffusivity, and poor electronic conductivity. Unlike $Al_2O_3$, LiPON is an excellent Li-ion conductor; it enables a relatively thick coating and is significantly effective in limiting electron migration. In conclusion, LiPON is expected to reduce interfacial resistance and demonstrate excellent properties in long cycles.

**Keywords: All solid state batteries, $Al_2O_3$ interface coating, Stability voltage window, Silicon alloy, Polyacrylonitrile coating, Radio frequency magnetron sputtering, LiPON interface coating**

**Student Number:** 2014-21440

# Table of Contents

# List of Figures

# Chapter 1. Introduction

## 1.1. Background of Study

### 1.1.1. Research objectives

Lithium-ion (Li-ion) batteries have various applications, spanning from small electronic devices to electric vehicles (EVs), owing to their high energy density, high operating voltage, good rate capability, long cycle life, and low self-discharge rate [1-6]. Generally, although graphite has been used as the anode material, it has a small theoretical capacity (372 mAh $g^{-1}$ for the $LiC_6$ phase). Among the promising materials for advanced anodes, silicon (Si) stands out with its high theoretical capacity (3,578 mAh $g^{-1}$ for the $Li_{15}Si_4$ phase), low cost, and natural abundance. The potential difference with lithium ion is 0.05 V for graphite, but silicon is 0.4 V. Accordingly, Si has the advantage of increasing the potential difference of the battery and preventing Li deposition [7-11]. However, Si has some disadvantages, including low electronic conductivity, low Li-ion diffusion coefficient, and large volume change (>300%) during Li insertion and extraction processes. These factors result in structural degradation, such as pulverization and cracks in Si, continuous electrolyte consumption, and reduced electrical contact with the current collector. Additionally, repetitive accumulation of the solid electrolyte interphase (SEI) layer increases the consumption of lithium ions. Consequently, the electrochemical performance of the electrode quickly deteriorates [12-15].

### 1.1.2. Silicon alloying

Several strategies have been implemented to improve the cycle performance of Li-ion batteries with a Si anode. Some reports proposed that a commercially available powder comprising active (Si) and inactive ($\alpha$-$FeSi_2$) alloys enhances the electronic conductivity and reduces the extent of volume changes, which improves the cycling capability of the anode. Inactive materials do not participate in the electrochemical reaction. The alloy powder was manufactured through a mechanical alloying process using a ball mill [16-20]. The ball-milled Si alloy powder, provided by the MKE company (Republic of Korea), was utilized as a starting material. It comprises finely dispersed powder of nanocrystalline Si and iron silicide ($\alpha$-$FeSi_2$). The D50 and D90 of the Si alloy powder are 2.98 and 5.24 μm, respectively.

### 1.1.3. Polyacrylonitrile coating

Carbon coating protects Si particles from contact with the electrolyte and can increase the electrical conductivity, resulting in a significant improvement in cycling performance [21, 22]. Among different carbon-types, polyacrylonitrile (PAN), a linear insulating polymer containing intrinsic triple-bonded nitrile groups, possesses unique properties. Before high-temperature carbonization, PAN undergoes cyclization in an inert environment. Cyclized PAN (cPAN) has a ladder structure containing both $sp^2$ hybridized C=C (C=N) bonds and $sp^3$ hybridized C-C(C-N) bonds when PAN is heat treated at a relatively low temperature [23, 24]. This low temperature cyclization allows the PAN to introduce delocalized $sp^2$ bonding in its conjugated pyridinic rings for electronic conductivity [25]. Therefore, heat-treatment is critical in transforming the PAN into a strong adhesion and conformal coating in the anode.

## 1.2. Radio-frequency Magnetron sputtering

Magnetron sputtering is a high-rate vacuum coating technique, known for its numerous advantages, including high coating efficiency, large coating area, precise control, a wide range of materials, and production of films with strong adhesion. In particular, radio-frequency (RF) magnetron sputtering offers high-frequency alternating current. Accordingly, RF sputtering can deposit conductors, semiconductors, and insulators. In addition, magnetron sputtering, which is performed by controlling power, gas ratio, and time, can be applied to powder coating and fully fabricated anodes. In addition, this coating technique can be used in battery materials [26].

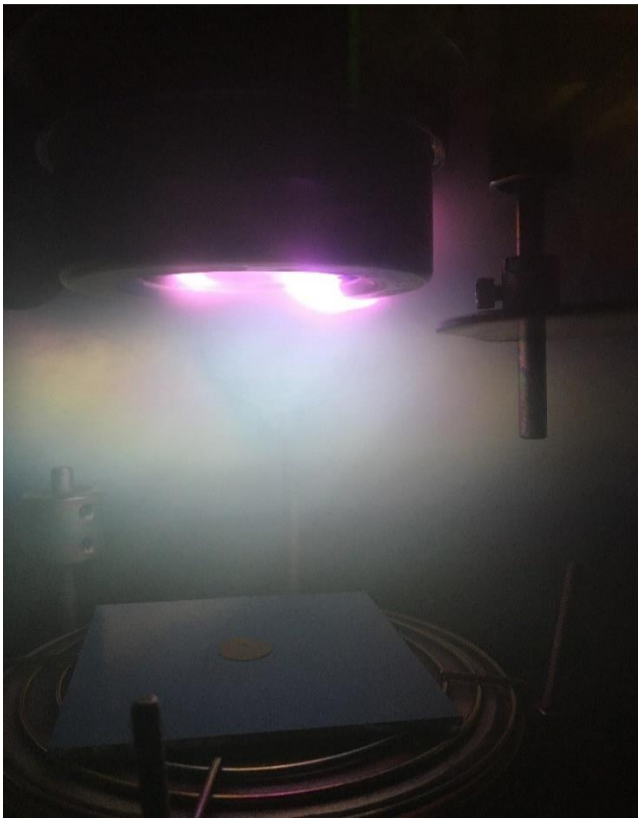

Figure 1.1. Radio-frequency sputtering system.

## 1.3. Microstructure analysis

The microstructure analysis of a battery is essential for understanding the mechanism by which its performance deteriorates during charge and discharge cycles. As lithium ions are sensitive to air, analysis can be conducted without air exposure using a focused ion beam (FIB) air lock chamber, suitable for Li ion battery analysis. Samples were prepared using a dual-beam FIB system (FEI, Nova NanoLab 200) to investigate the sample microstructure. Cross-sections and images before and after cyclized powders or electrodes were obtained using a dual-beam FIB. In addition, electrodes were cross-sectioned to show their volumetric expansion after cycles. The sample preparation process for transmission electron microscopy (TEM) is as follows: platinum is deposited onto a region of interest to prevent damage to the surface layer by the Ga ion beam. FIB milling using Ga ions creates a cross-section. Subsequently, the cutoff sample is lifted out, attached to a TEM grid, and fine-milled to a proper thickness of approximately 50 nm. TEM samples were prepared using a FIB's 30 keV Ga ion beam. Materials analysis was performed using a JEOL ARM200F FEG-TEM/STEM operated at 200 keV. All preparations must occur under an inert environment, owing to the utmost air sensitivity of the samples.

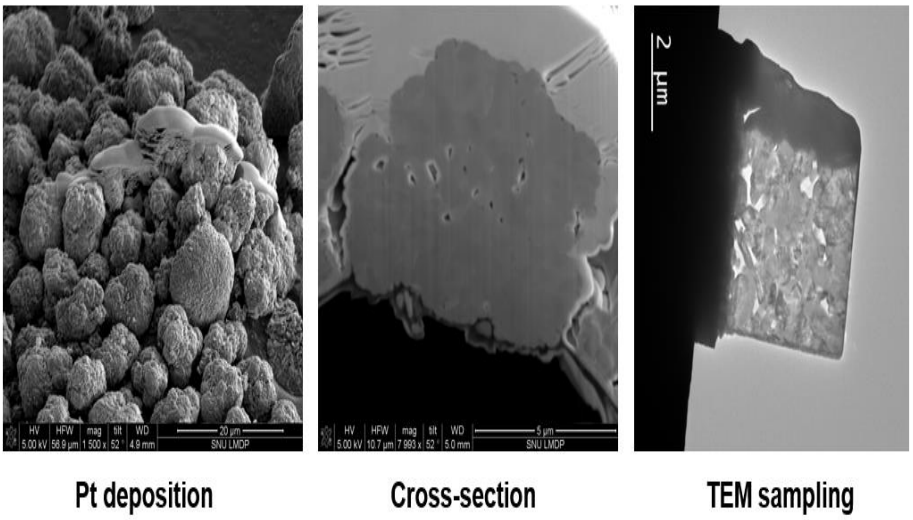


Figure 1.2. Sample preparation process for transmission electron microscopy (TEM) using FIB-SEM.

## 1.4. References

[1] J.-M. Tarascon, M. Armand, Issues and challenges facing rechargeable lithium batteries, Nature 414 (2001) 359–367.

[2] M. Armand, J.-M. Tarascon, Building better batteries, Nature 451 (2008) 652–657.

[3] R. Marom, S.F. Amalraj, N. Leifer, D. Jacob, D. Aurbach, A review of advanced and practical lithium battery materials, J. Mater. Chem. 21 (2011) 9938–9954.

[4] R.A. Huggins, Alternative materials for negative electrodes in lithium systems, Solid State Ionics 152 (2002) 61–68.

[5] Y.-P. Wu, E. Rahm, R. Holze, Carbon anode materials for lithium ion batteries, J. Power Sources 114 (2003) 228–236.

[6] B. Scrosati, J. Garche, Lithium batteries: status, prospects and future, J. Power Sources 195, 2419 (2010).

[7] R. Marom, S. F. Amalraj, N. Leifer, D. Jacob, and D. Aurbach, A review of advanced and practical lithium battery materials, J. Mater. Chem. 21, 9938 (2011).

[8] J.-Y. Li, Q. Xu, G. Li, Y.-X. Yin, L.-J. Wan, Y.-G. Guo, Research progress regarding Si- based anode materials towards practical application in high energy density Li-ion batteries, Mater. Chem. Front. (2017).

[9] W.-J. Zhang, A review of the electrochemical performance of alloy anodes, J. Power Sources 196, 13 (2011).

[10] D. Ma, Z. Cao, A. Hu, Si-based anode materials for Li-ion batteries: a mini review, Nano-Micro Lett. 6 (2014) 347–358.

[11] M. N. Obrovac and V. L. Chevrier, Alloy negative electrodes for Li-ion batteries, Chem. Rev. 114, 11444 (2014).

[12] A. R. Kamali and D. J. Fray, Review on carbon and silicon-based materials as anode materials for lithium ion batteries, J. New Mat. Electrochem. Systems 13, 147 (2010).

[13] C.-M. Park, J.-H. Kim, H. Kim, H.-J. Sohn, Li-alloy based anode materials for Li secondary batteries, Chem. Soc. Rev. 39 (8) (2010) 3115–3141.

[14] J.H. Ryu, J.W. Kim, Y.-E. Sung, S.M. Oh, Failure modes of silicon powder negative electrode in lithium secondary batteries, Electrochem. Solid-State Lett. 7 (10) (2004) A306–A309.

[15] H. Wu and Y. Cui, Designing nanostructured Si anodes for high energy lithium ion batteries, Nano Today 7, 414 (2012).

[16] N. Fukata, M. Mitome, Y. Bando, W. Wu, and Z. L. Wang, Lithium ion battery anodes using Si-Fe based nanocomposite structures, Nano Energy 26, 37 (2016).

[17] Y. Chen, J. Qian, Y. Cao, H. Yang, and X. Ai, Green Synthesis and Stable Li-Storage Performance of $FeSi_2$ /Si@C Nanocomposite for Lithium-Ion Batteries, ACS Appl. Mater. Interfaces 4, 3753 (2012).

[18] M. D. Fleischauer, J. M. Topple, and J. R. Dahn, Combinatorial investigations of Si-M (M = Cr + Ni, Fe, Mn) thin film negative electrode materials, Electrochem. Solid-State Lett. 8, A137 (2005).

[19] B. Zhu, Y. Jin, Y. Tan, L. Zong, Y. Hu, L. Chen, Y. Chen, Q. Zhang, J. Zhu, Scalable production of Si nanoparticles directly from low grade sources for lithium-ion battery anode, Nano Lett. 15 (2015) 5750–5754.

[20] K. K. Lee, J. J. Jeong, Y. E. Chu, J. B. Kim, K. H. Oh, J. T. Moon, Properties of Fe–Si Alloy Anode for Lithium-Ion Battery Synthesized Using Mechanical Milling, MDPI Materials, 15 (2022) 1873.

[21] M. Yoshio, H. Wang, K. Fukuda, Y. Hara, Y. Adachi, Effect of carbon coating on electrochemical performance of treated natural graphite as lithium-ion battery anode material, J Electrochem Soc. 147 (2000) 1245–1250.

[22] N. Dimov, S. Kugino, M. Yoshio, Carbon-coated silicon as anode material for lithium ion batteries: advantages and limitations, Electrochim Acta 48 (2003) 1579–1587.

[23] R. Janus, P. Natkanski, A. Wach, M. Drozdek, Z. Piwowarska, P. Cool, P. Kustrowski, Thermal transformation of polyacrylonitrile deposited on SBA-15 type silica Effect on adsorption capacity of methyl–ethyl ketone vapor, J. Therm. Anal. Calorim. 110 (2012) 119.

[24] M. S. A. Rahaman, A. F. Ismail, A. Mustafa, A review of heat treatment on polyacrylonitrile fiber Polym. Degrad. Stab. 92 (2007) 1421.

[25] D. M. Piper, T. A. Yersak, S. B. Son, S. C. Kim, C. S. Kang, K. H. Oh, C. Ban, A. C. Dillon, and S. H. Lee, Conformal Coatings of Cyclized-PAN for Mechanically Resilient Si nano-Composite Anodes, Adv. Energy Mater. 3 (2013) 697.

[26] Y. Ma, L. Li, J. Qian, W. Qu, R. Luo, F. Wu, R. Chen, Materials and structure engineering by magnetron sputtering for advanced lithium batteries, Energy Storage Materials 39 (2021) 203–224.

# Chapter 2. Improved Cycle Properties of All-Solid-State Li-Ion Batteries with $Al_2O_3$ Coating on the Silicon-Based Anode

## 2.1. Introduction

Over the past decade, lithium-ion batteries (LIBs) have become quite popular in our society, from small electronic devices to electric vehicles. As the demand for electric vehicles with high energy density increases, LIBs with high safety ratings and energy densities will be required [1-6]. Conventional LIBs use organic liquid electrolytes, which are highly flammable and have energy density challenges [7, 8]. Battery safety can be improved with the use of solid electrolytes, which substitute volatile organic liquid electrolytes for a stable solid electrolyte. Solid-state electrolytes also serve as a battery separator; Addition of the active materials increases the energy density. In addition, all-solid-state batteries can operate over a broad temperature range, enabling the use of batteries in extreme conditions [9, 10].

There has been extensive research on solid electrolytes for all solid-state batteries [11]. Many scientists agree that the interfacial resistance of all-solid-state Li-ion batteries has become a major performance barrier. A high energy density solid-state battery must have a wide electrochemical-stability window. The stability window voltage of an electrolyte refers to the voltage range it can maintain without breakdown [12-14].

Recently, the electrochemical stability of various solid electrolytes in all-solid-state Li-ion batteries was investigated by first-principles calculations [15, 16]. This explains why sulfide-based electrolytes have a small thermodynamic intrinsic electrochemical stability in the range of 1.7–2.3 V (compared to $Li^+$/Li). With low voltage, sulfide electrolytes tend to be reduced on the anode surface. Although the solid sulfide electrolyte exhibits high ionic conductivity, interfacial breakdown of sulfide solid electrolytes occurs on the anode surfaces, resulting in increased interfacial resistance and reduced electrochemical performance [17-19].

Applying interfacial coating layers is a simple and effective method to address the interfacial challenges. Coatings between the solid electrolyte and the electrode should extend the electrolytes' stable voltage window and allow for Li-ion conduction but not electron conduction. The passivating layer can prevent or slow down solid electrolyte decomposition [20-21]. The artificial $Al_2O_3$ layer alters the ion-conductive Li–Al–O layer upon lithiation, which not only provides a pathway for Li-ion transport but also acts as a physical barrier to stop side reactions between the electrolyte and anode. The Li–Al–O has a lower reduction potential than the sulfide solid electrolyte ($Li_5AlO_4$ (0.06V), $LiAlO_2$ (0.17V), and $LiAl_5O_8$ (0.81V)) [17]. The $Al_2O_3$ coating's capacity retention enhancement is attributed to a reduction in the electrolyte reduction process and lithium loss associated with stable solid electrolyte interphase (SEI) formation.

Recently, several studies have showed that Si thin film [22] or $TiO_2$ nanotube [23] coated with $Al_2O_3$ in liquid electrolyte demonstrated enhanced cycling performance and prevented side reaction. In addition, a variety of researchers have exhibited that $Al_2O_3$ coating on Li metal foil [24] or Sn particles [25] in solid electrolyte results in better longer cycling performance of batteries. The addition of $Al_2O_3$ to the solid electrolyte improves the stability of the solid electrolyte and broadens the electrochemical-stability window. Deng et al. shows an outstanding cycling performance by synthesizing $Li_{6.75}La_3Zr_{1.75}Ta_{0.25}O_{12}$ (LLZTO) and $Al_2O_3$ [26]. Zhou et al. present nanocomposite $Li_2B_{12}H_{12}$-$Al_2O_3$ that has a wider electrochemical-stability and voltage windows and improved compatibility with the anode and cathode [27]. In the present study, we have successfully applied strategies such as $Al_2O_3$ coating directly on Si-based anode in a sulfide solid electrolyte. A simple and efficient interface engineering was applied to a sulfide-base solid electrolyte with high ionic conductivity but a narrow electrochemical-stability window. Two-dimensional (2D) thin film coating decreases the electrolyte reduction reaction and the loss of lithium associated with SEI formation, resulting in considerable improvements in the cycling performance. This work leads to the development of a novel silicon-based anode all-solid-state battery.

## 2.2. Material and methods

### 2.2.1. Polyacrylonitrile coating on Si alloy

The starting material was ball-milled silicon alloy powder supplied by MKE company (Republic of Korea). It consists of nanocrystalline silicon and iron silicide (α-$FeSi_2$) distributed in a fine powder. The D50 and D90 values for powder silicon alloy are 2.98 and 5.24 μm, respectively. In previous work [28], the preparation of this ball-milled Si alloy powder was disclosed. According to some reports, a commercially available powder exists that consists of active (Si)/inactive (iron silicide) alloys, which improves the anode's cycling capabilities by increasing electronic conductivity and decreasing the magnitude of volume fluctuations [29-32].

The composite anode materials were made by combining 32 mg of polyacrylonitrile (PAN) powder (average MW 150,000, Sigma-Aldrich, United States) with 350 mg of N,N-dimethylformamide (DMF) solvent (Fisher Scientific, United States) using a Speed Mixer (DAC 330-100 PRO, Flacktek, United States). Then 96 mg of the active material (D (0.5) = 2.98 μm, MKE, Republic of Korea) was added and thoroughly mixed to dissolve the PAN and disperse the silicon iron composite uniformly. This slurry was evenly distributed onto copper foil and dried at 60 ℃ in a vacuum oven. From the electrode sheet, 12 mm diameter electrodes were cut and then heat-treated in an argon-filled tube furnace. The tube furnace is heated for 3 h at 270 ℃. The temperature was then maintained for 3 h before cooling to room temperature.

Carbon coating is observed to protect Si particles from electrolyte contact and thus increases their electrical conductivity, thereby improving the cycling performance [33, 34]. Polyacrylonitrile (PAN) is a linear insulating polymer containing nitrile groups that are intrinsically triple-bonded, and its electronic conductivity is dependent on the heat-treatment temperature. Prior to carbonization at high temperatures, PAN undergoes cyclization in an inert environment. Cyclized PAN (cPAN) is characterized by a ladder structure, comprising $sp^2$ hybridized C=C (C=N) links and $sp^3$ hybridized C–C (C–N) bonds [35, 36]. This low-temperature cyclization introduces delocalized $sp^2$ bonds to the conjugated pyridinic rings of PAN, conferring electronic conductivity without reducing the polymeric toughness of PAN [37].

### 2.2.2. $Al_2O_3$ coating on the anode

Radio frequency (RF) sputtering can be used to deposit conductors, semiconductors, and insulators. RF magnetron sputtering provides high-frequency alternating. Magnetron sputtering is a rapid vacuum coating technique and possesses a number of benefits including excellent coating efficiency, a large coating area, precise control, the ability to use a wide range of materials, and the production of films with strong adhesion. This coating process is also applicable to battery materials [38].

$Al_2O_3$ layers were deposited on a Si-based anode by RF magnetron sputtering of a 99.99% pure aluminum (Plasmaterials, United States) target in an Ar and $O_2$ atmosphere. The sputtering was performed at a fixed power (50 W), and the distance between the target and substrate was also fixed at 5.0 ㎝. Within the sputtering chamber, a punched Si alloy/cPAN anode was placed on a glass plate. Before sputtering, Ar gas (20 SCCM) was added to the chamber and the target was pre-sputtered for 10 minutes at 50 W to remove surface contamination. Adjustments were made to the Ar and $O_2$ gas flows into the chamber (18 and 2 SCCM, respectively) while maintaining the chamber pressure at $8.3 \times 10^{-3}$ mTorr. Changing the deposition time varied the thickness of the $Al_2O_3$ layer, resulting in a thin coating on the anode. RF magnetron sputtering improved the electrochemical performance of the $Al_2O_3$-coated anode by varying the $Al_2O_3$ layer thickness.

### 2.2.3. All-solid-state half-cell constructions

Figure 1 shows the polyetheretherketone (PEEK) split cell. The anode, sulfide solid electrolyte, and InLi were placed in the polymer mold. The half cell were then inserted into the mold and compacted into a tablet with a hydraulic press. The half-cells were constructed and tested in the dry environment of a glovebox that is filled with argon gas. For the assembly and cycling of the half-cells, 13 mm diameter titanium cell dies coated with PEEK were used. Due to their mechanical strength and broad electrochemical-stability window, titanium plungers that have been polished were used as current collectors. As a solid-state electrolyte (SSE) powder, 150 mg of amorphous $77.5Li_2S$-$22.5P_2S_5$ was placed over a Si-based anode and compressed with a hydraulic press less than one ton of force for three minutes. The $77.5Li_2S$-$22.5P_2S_5$ SSE was prepared by mechanochemically reacting stoichiometric quantities of $Li_2S$ (Aldrich, 99.9%) and $P_2S_5$ (Aldrich, 99%) using a planetary ball mill (MTI, United States). As a counter electrode, 50 mg of a lithium–indium (InLi) alloy was evenly distributed and pressed at a force of five tons for five minutes; 99.999% indium (Alfa Aesar, United States) and lithium (FMC Lithium, United States) powders were mixed in a vial using a Vortex Genie2 (Scientific Industries, United States) to produce the InLi alloy with a potential of 0.62 V versus Li+/Li [39].

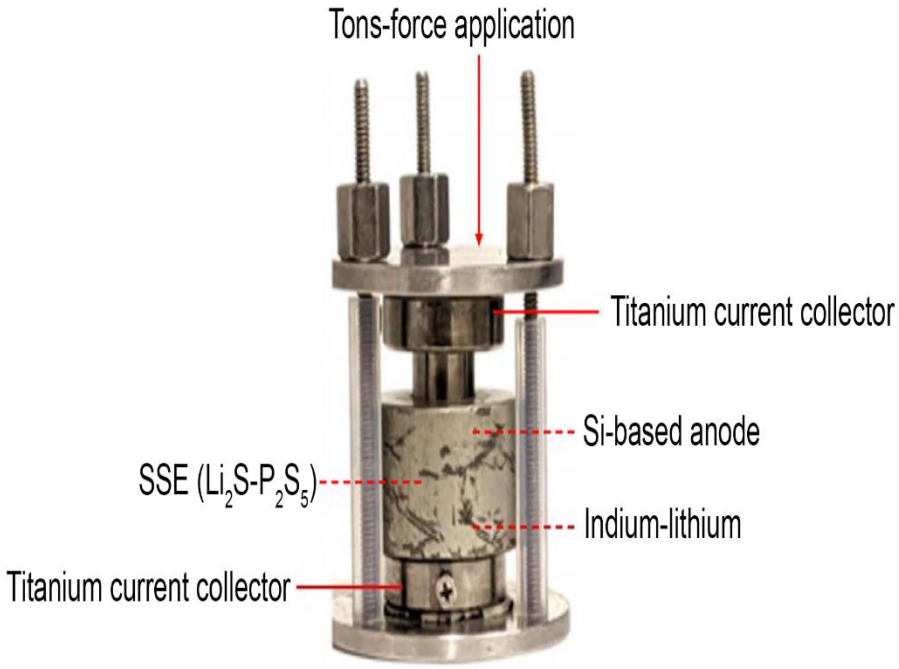


Figure 2.1. Assembly of the polyetheretherketone split cell.

### 2.2.4. Electrochemical measurements

The all-solid-state half-cells were cycled at 60 °C using an Arbin 2000 battery test station (Arbin Instruments, United States) and a constant current, constant voltage testing protocol. To achieve full delithiation of the Si alloy composite electrodes, each half-cell was cycled within a voltage window of 5 mV–1.5 V versus Li+/Li, with a one-hour voltage hold at the upper voltage limit. During testing, each cell was maintained at 60 °C with a 20 MPa compressive clamping force in an argon atmosphere. This small external compressive stress was applied to the contact between the electrodes of the half-cells and the titanium plunger of the cell die [40]. By determining the approximate Si content in each composite electrode, the half-cells were subjected to a C/20 cycle (1st cycle) and C/10 cycles (2-100cycles) assuming 100% silicon utilization.

Using a Biologic VSP (LAMBDA system, Polska), electrochemical impedance spectroscopy (EIS) was carried out on the Si alloy–PAN-coated (Si alloy–PAN|a77.5|InLi) and Si alloy–PAN–$Al_2O_3$-coated (Si alloy–PAN-$Al_2O_3$|a77.5|InLi) all-solid-state cells after the 100 cycles of delithiation. The EIS scans (0.01-3000000 Hz, 10 mV AC amp., open-circuit-potential) were conducted at room temperature after the $100^{th}$ (delithiation) to 1 V. At 60 °C, the cells completed an initial C/20 conditioning cycle (5 mV–1.5 V) followed by a second C/10 conditioning cycle (5 mV–1.5 V) [41].

### 2.2.5. Rate capability measurements

The half-cells were cycled at 60 °C using an Arbin 2000 battery test station and a symmetric constant voltage protocol. The half-cells were initially subjected to a C/20 cycle (50 mV–1.5 V, vs. Li/Li+) before being cycled at increasing rates within a set voltage window of 50 mV–1.5 V, vs. Li/Li+. On the cathode side, 60 mg of a lithium-indium (InLi) alloy was used.

### 2.2.6. Material characterization

To explore the microstructure of the anode, Si alloy-cPAN-$Al_2O_3$-coated electrodes were prepared using a dual-beam focused ion beam (FIB, FEI, Nova Nanolab 200). The FIB was utilized to cross-section and scan Si alloy–PAN–$Al_2O_3$-coated electrodes. Samples for transmission electron microscopy (TEM) were prepared using the FIB's 30 keV Ga+ ion beam and a JEOL ARM200F FEG-TEM/STEM, operating at 200 kV was used to analyze the anode's chemical composition. $Al_2O_3$ was analyzed using TEM-energy-dispersive X-ray spectroscopy (TEM-EDS). Due to the air-sensitive nature of all the samples, the samples were prepared in an inert environment.

### 2.2.7. Theory

The stability-voltage window of an electrolyte defines the voltage range over which the electrolyte is not decomposed by oxidation or reduction. Sulfide-based electrolytes have high ionic conductivity but a narrow electrochemical-stability window. Decomposition of the sulfide solid electrolyte on the anode surface increases the interfacial resistance and degrades the electrochemical performance. When an $Al_2O_3$ coating is applied to the electrolyte–anode interface, it reacts with Li to form a Li–Al–O layer that lowers the reduction voltage and inhibits the solid electrolyte decomposition. Although the cell operates with an Si alloy–PAN, the simple $Al_2O_3$ coating reduces the side reaction of the electrolyte and changes the properties of the interface contacting the solid electrolyte.

## 2.3. Results and Discussion

### 2.3.1. Results

Figure 2 presents the TEM micrographs of the $Al_2O_3$-coated anode (1 min, 50 W) before cycling. In an energy dispersive X-ray spectroscopy (EDX) elemental line scan, the thin aluminum oxide coating layer was identified. The line scan generated from the anode's surface reveals the existence of aluminum.

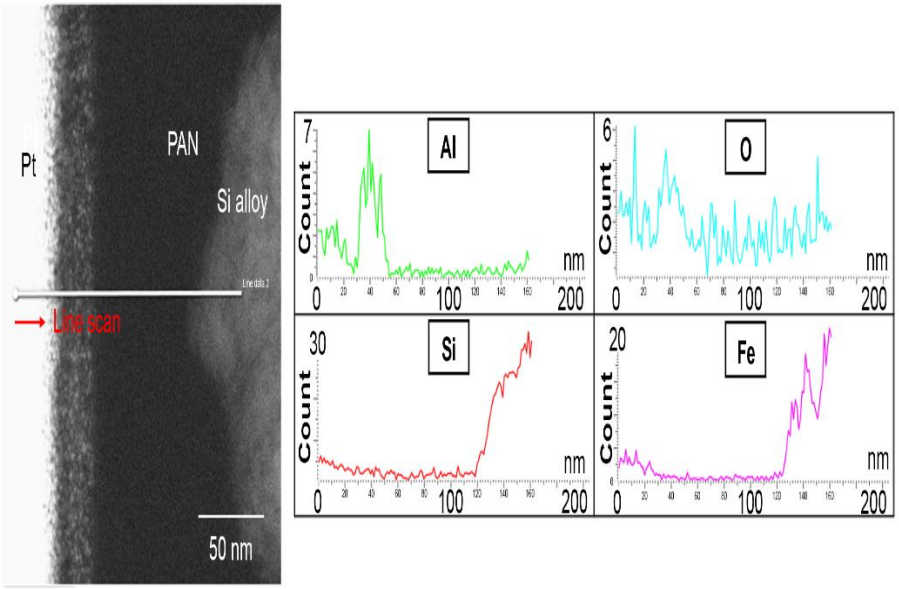


Figure 2.2. TEM-EDS line scan of $Al_2O_3$-coated anode: 50 W, 1 min.

The half-cell anodes were fabricated from the Si alloy–PAN with varying $Al_2O_3$ thicknesses. Figure 3 shows the discharge/charge capacities of the anodes as functions of cycle number. The $Al_2O_3$ coating applied for 1 min (green line) achieved the best cycle performance. The performance of anodes coated with $Al_2O_3$ for 0.5 min (red line) and 2.5 min (blue line) were lesser than that of the 1-min-coated sample, but they outperformed the uncoated anode (black line). Therefore, the cycle characteristics were dependent on the thickness of the $Al_2O_3$ coating. The initial discharge/charge capacity of the Si alloy–PAN sample (pristine) was 1207.8/897 mAh $g^{-1}$, with an initial coulombic efficiency (CE) of 74.3%. Whereas, $Al_2O_3$ coating (1 min, 50 W) delivered an initial discharge/charge capacity of 1239.6/941.3 mAh $g^{-1}$, improving the initial coulombic efficiency to 75.9%. Thus, $Al_2O_3$ slightly improved the initial coulombic efficiency compared with the pristine sample owing to its thinness. An increased electronic conductivity of the PAN stimulated its electron-tunneling capability, further reducing the solid electrolyte. As the instability of the SEI increased, the capacity retention of the pristine anode declined to 34.3% after 100 cycles, whereas that of anode with the $Al_2O_3$ (1 min, 50 W) coating was 58.9%. Echoing the cycling performance, the capacity retention decreased rapidly in the pristine composite anode sample but was retained for much longer in the $Al_2O_3$ (1 min, 50 W)-coated anode over 100 cycles [42].

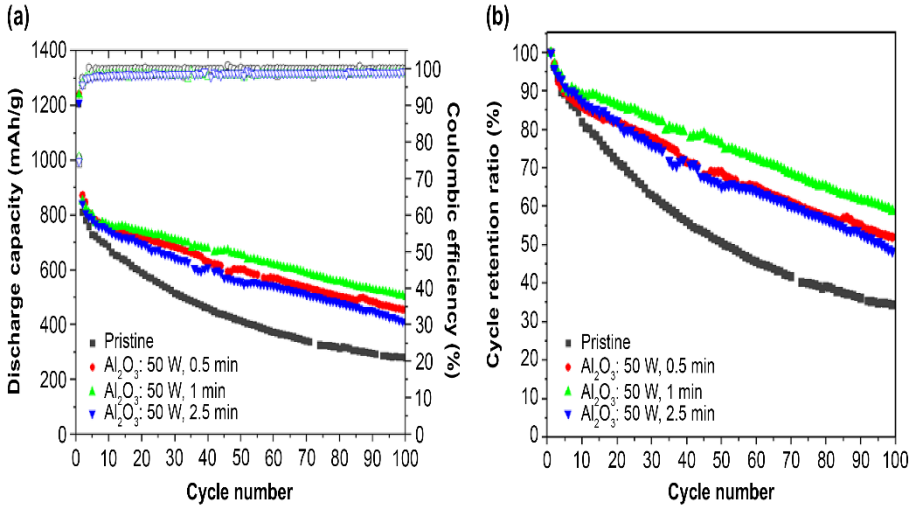


Figure 2.3. (a) Discharge capacity of Pristine and $Al_2O_3$-coated anodes.

(b) Cycle retention ratio of pristine and $Al_2O_3$-coated anodes.

The rate capability of the $Al_2O_3$ (1 min, 50 W) and pristine samples was also evaluated in Figure 4. The rate capability was increased from 0.1 C to 0.5 C before it was reduced to 0.2 C. $Al_2O_3$ (1 min, 50 W) exhibited higher capacity retention than pristine past rates of 0.2 C. This suggests that the SEI layer of the $Al_2O_3$-coated anode was stable and not susceptible to damage at that rate.

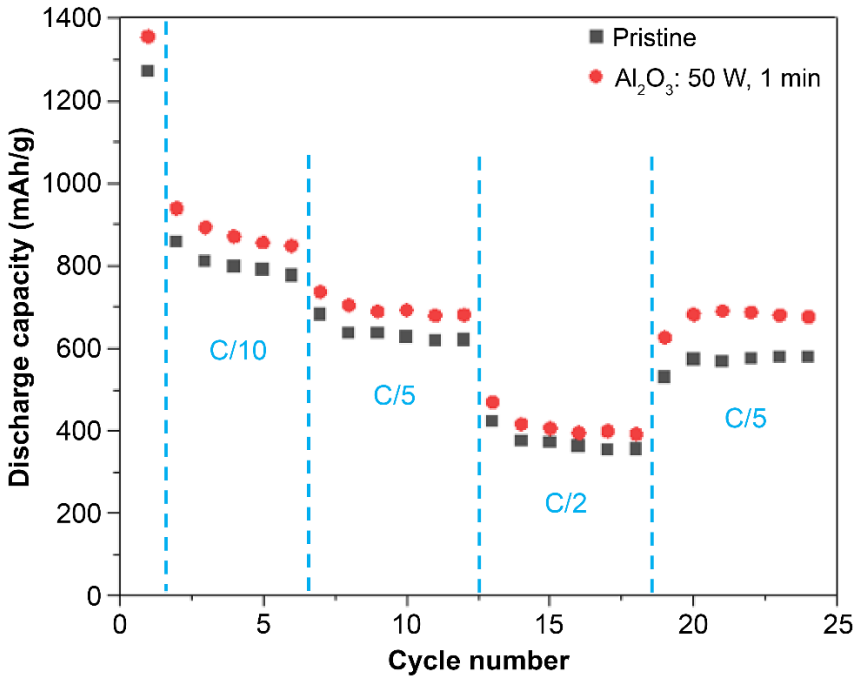


Figure 2.4. Rate capability test of the Pristine and $Al_2O_3$-coated anodes: 50 W, 1 min.

Figure 5 shows the differential capacity (dQ/dV) plots of the $Al_2O_3$ (1 min, 50 W) and pristine samples. During the first discharge (lithiation) and charge (delithiation) cycle, the typical voltage profiles were related to the lithiation/delithiation reaction of silicon and lithium. The only difference between the pristine and $Al_2O_3$ (1 min, 50 W)-coated anode was a small peak, so it was assumed to be corresponding to the reaction peak of aluminum and Li. In the voltage profile (Figure 6), the delithiation of the $Al_2O_3$-coated sample displays better charge–discharge overlapping and reaction reversibility than the pristine anode.

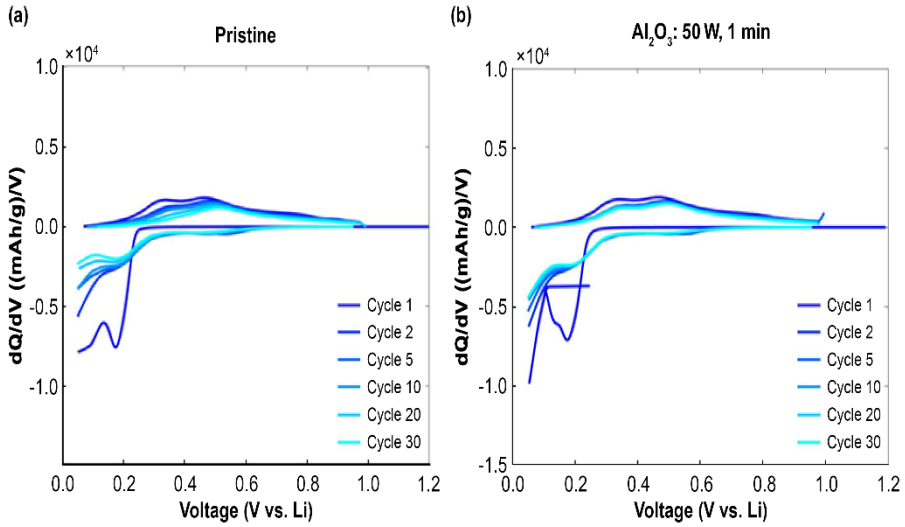


Figure 2.5. Differential capacity of the (a) pristine and (b) $Al_2O_3$-coated anodes: 50 W, 1 min.

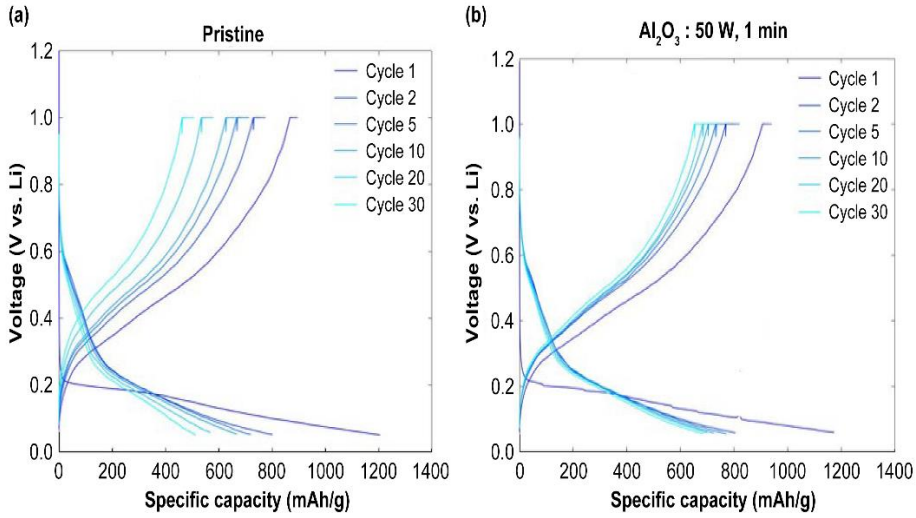


Figure 2.6. Voltage profile of the (a) pristine and (b) $Al_2O_3$-coated anodes: 50 W, 1 min.

To better understand the surface-layer effects of the $Al_2O_3$ coating, the $Al_2O_3$ (1 min, 50 W)-coated and pristine anodes were subjected to an ESI analysis after 100 cycles. Figure 7 plots the imaginary part (Z'') versus the real part (Z') of the anode impedances. The semicircles in the medium-frequency region correspond to the charge-transfer resistance ($R_{CT}$) at the electrode–electrolyte interfaces. The $R_{CT}$ of the $Al_2O_3$ (1 min, 50 W)-coated anode was 57.16 Ω compared with 93.26 Ω for the pristine anode. The lower charge-transfer resistance of the $Al_2O_3$ (1 min, 50 W)-coated electrode than that of the pristine electrode can be attributed to the Li–Al–O surface layer formed at the electrode–electrolyte interface. These EIS results are in excellent agreement with the cyclic performances (Figure 3) and the rate capabilities (Figure 4). The more the amount of decomposed electrolytes, the thicker will be the SEI and more will be the charge-transfer resistance at the interface.

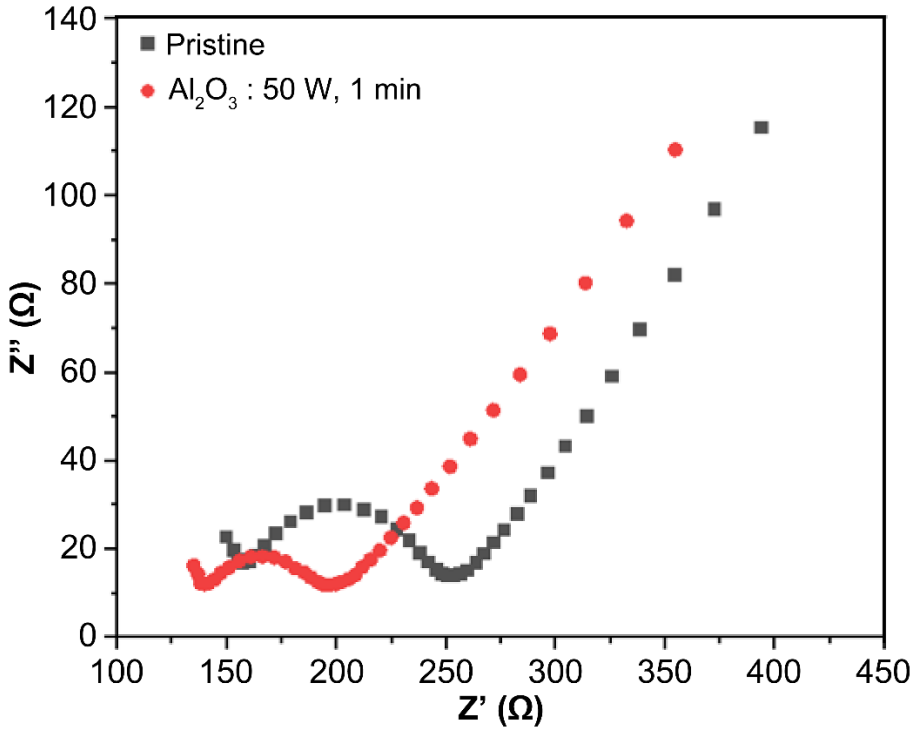


Figure 2.7. EIS results of the pristine and $Al_2O_3$-coated anodes: 50 W, 1 min at 100 cycles.

### 2.3.2. Discussion

The $Al_2O_3$ coating layer transformed into an artificial ion-conductive Li–Al–O layer, which not only improved the diffusion of Li+ through the Li–Al–O layer but also acted as a barrier to prevent the electron transport between the anode and the solid electrolyte [43-45]. The appropriate $Al_2O_3$ coating thickness decreases the regeneration of a thick SEI film on the electrode and also decreases the consumption of Li-ions during lithiation/delithiation

## 2.4. Conclusion

In this work, a Si alloy–PAN anode was prepared using an $Al_2O_3$ coating as an artificial SEI layer and was applied by RF plasma. In all-solid-state LIBs, the electrochemical properties of the $Al_2O_3$-coated half-cells were enhanced. After 100 cycles, the $Al_2O_3$-coated anode (coated for one minute) retained 58.86% of its capacity, while the uncoated $Al_2O_3$ anode retained 34.34% of its capacity. This much-improved electrochemical property is attributed to the $Al_2O_3$ coating. An appropriate $Al_2O_3$ coating reduces the resistance at the interface, effectively inhibits electrolyte decomposition and suppresses the formation of an additional SEI layer, reducing Li-ion consumption and improving cycle characteristics. This study presented a method to lower the interfacial resistance through interfacial coating, and results of this study can lead to the wide spread use of sulfide-based electrolytes through interfacial coating of potential materials with artificial SEI.

## 2.5. References

[1] J.M. Tarascon, M. Armand, Issues and challenges facing rechargeable lithium batteries, Nature 414 (2001) 359–367.

[2] M. Armand, J.M. Tarascon, Building better batteries, Nature 451 (2008) 652–657.

[3] R. Marom, S.F. Amalraj, N. Leifer, D. Jacob, D. Aurbach, A review of advanced and practical lithium battery materials, J. Mater. Chem. 21 (2011) 9938–9954.

[4] R.A. Huggins, Alternative materials for negative electrodes in lithium systems, Solid State Ionics 152–153 (2002) 61–68.

[5] B. Scrosati, J. Garche, Lithium batteries: status, prospects and future, J. Power Sources 195 (2010) 2419–2430.

[6] J.-Y. Li, Q. Xu, G. Li, Y.-X. Yin, L.-J. Wan, Y.-G. Guo, Research progress regarding Si-based anode materials towards practical application in high energy density Li-ion batteries, Mater. Chem. Front. 1 (2017) 1691–1708.

[7] S.S. Zhang, Liquid electrolyte lithium/sulfur battery: Fundamental chemistry, problems, and solutions, J. Power Sources 231 (2013) 153–162.

[8] S.S. Zhang, A review on the separators of liquid electrolyte Li-ion batteries, J. Power Sources 164 (2007) 351–364.

[9] A. Manthiram, X. Yu, S. Wang, Lithium battery chemistries enabled by solid-state electrolytes, Nat. Rev. Mater. 2 (2017) 16103.

[10] B. Zheng, X. Liu, J. Zhu, J. Zhao, G. Zhong, Y. Xiang, H. Wang, W. Zhao, E. Umeshbabu, Q.-H. Wu, J. Huang, Y. Yang, Unraveling (electro)-chemical stability and interfacial reactions of $Li_{10}SnP_2S_{12}$ in all-solid-state Li batteries, Nano Energy 67 (2020) 104252.

[11] W. Zhao, J. Yi, P. He, H. Zhou, Solid-state electrolytes for lithium-ion batteries: Fundamentals, challenges and perspectives, Electrochem. Energy Rev. 2 (2019) 574–605.

[12] Y. Su, J. Hao, X. Liu, Y. Yang, Progress of atomic layer deposition and molecular layer deposition in the development of all-solid-state lithium batteries, Batteries Supercaps 6 (2023) e202200359.

[13] Y. Zhao, K. Zheng, X. Su, Addressing Interfacial Issues in liquid-based and solid-state batteries by atomic and molecular layer deposition, Joule 2 (2018) 2583–2604.

[14] Y. Li, D. Zhang, X. Xu, Z. Wang, Z. Liu, J. Shen, J. Liu, M. Zhu, Interface engineering for composite cathodes in sulfide-based all-solid-state lithium batteries, J. Energy Chem. 60 (2021) 32–60.

[15] T.K. Schwietert, A. Vasileiadis, M. Wagemaker, First-principles prediction of the electrochemical stability and reaction mechanisms of solid-state electrolytes, JACS Au. 1 (2021) 1488–1496.

[16] Y. Zhu, X. He, Y. Mo, First principles study on electrochemical and chemical stability of solid electrolyte–electrode interfaces in all-solid-state Li-ion batteries, J. Mater. Chem. A. 4 (2016) 3253–3266.

[17] S. Yu, H. Park, D.J. Siegel, Thermodynamic assessment of coating materials for solid-state Li, Na, and K batteries, ACS Appl. Mater. Interfaces 11 (2019) 36607–36615.

[18] Y. Zhu, X. He, Y. Mo, Origin of outstanding stability in the lithium solid electrolyte materials: Insights from thermodynamic analyses based on first-principles calculations, ACS Appl. Mater. Interfaces 7 (2015) 23685–23693.

[19] A. Banerjee, X. Wang, C. Fang, E.A. Wu, Y.S. Meng, Interfaces and Interphases in all-solid-state batteries with inorganic solid electrolytes, Chem. Rev. 120 (2020) 6878−6933.

[20] A. Neumann, S. Randau, K. Becker-Steinberger, T. Danner, S. Hein, Z. Ning, J. Marrow, F.H. Richter, J. Janek, A. Latz, Analysis of interfacial effects in all-solid-state batteries with thiophosphate solid electrolytes, ACS Appl. Mater. Interfaces. 12 (2020) 9277–9291.

[21] W.D. Richards, L.J. Miara, Y. Wang, J.C. Kim, G. Ceder, Interface stability in solid-state batteries, Chem. Mater. 28 (2016) 266–273.

[22] S. Casino, B. Heidrich, A. Makvandi, T. Beuse, T. Gallasch, M. Peterlechner, G. Wilde, M. Winter, P. Niehoff, $Al_2O_3$ protective coating on silicon thin film electrodes and its effect on the aging mechanisms of lithium metal and lithium ion cells, J. Energy Storage 44 (2021) 103479.

[23] H. Sopha, G.D. Salian, R. Zazpe, J. Prikryl, L. Hromadko, T. Djenizian, J.M. Macak, ALD $Al_2O_3$-coated $TiO_2$ nanotube layers as anodes for lithium-ion batteries, ACS Omega. 2 (2017) 2749–2756.

[24] L. Wang, L. Zhang, Q. Wang, W. Li, B. Wu, W. Jia, Y. Wang, J. Li, H. Li, Long lifespan lithium metal anodes enabled by $Al_2O_3$ sputter coating, Energy Storage Mater. 10 (2018) 16–23.

[25] X. Zhou, L. Stan, D. Hou, Y. Jin, H. Xiong, L. Zhu, Y. Liu, Operando study of mechanical integrity of high-volume expansion Li-ion battery anode materials coated by $Al_2O_3$, Nanotechnology 34 (2023) 235705.

[26] F. Deng, Y. Wu, W. Tang, S. Song, Z. Wen, M. Kotobuki, L. Lu, J. Yao, N. Hu, J. Molenda, Conformal, nanoscale γ-$Al_2O_3$ coating of garnet conductors for solid-state lithium batteries, Solid State Ionics 342 (2019) 115063.

[27] C. Zhou, H. Sun, Q. Wang, J.B. Grinderslev, D. Liu, Y. Yan, T.R. Jensen, Highly electrochemically stable $Li_2B_{12}H_{12}$-$Al_2O_3$ nanocomposite electrolyte enabling A 3.8 V room-temperature all-solid-state Li-ion battery, J. Alloys Compound 938 (2023) 168689.

[28] K.K. Lee, J.J. Jeong, Y.E. Chu, J.B. Kim, K.H. Oh, J.T. Moon, Properties of Fe–Si alloy anode for lithium-ion battery synthesized using mechanical milling, Materials 15 (2022) 1873.

[29] N. Fukata, M. Mitome, Y. Bando, W. Wu, Z.L. Wang, Lithium ion battery anodes using Si-Fe based nanocomposite structures, Nano Energy 26 (2016) 37–42.

[30] Y. Chen, J. Qian, Y. Cao, H. Yang, X. Ai, Green synthesis and stable Li-storage performance of $FeSi_2$ /Si@C nanocomposite for lithium-ion batteries, ACS Appl. Mater. Interfaces 4 (2012) 3753–3758.

[31] M.D. Fleischauer, J.M. Topple, J.R. Dahn, Combinatorial investigations of Si-M (M = Cr + Ni, Fe, Mn) thin film negative electrode materials, Electrochem. Solid-State Lett. 8, (2005) A137.

[32] B. Zhu, Y. Jin, Y. Tan, L. Zong, Y. Hu, L. Chen, Y. Chen, Q. Zhang, J. Zhu, Scalable production of Si nanoparticles directly from low grade sources for lithium-ion battery anode, Nano Lett. 15 (2015) 5750–5754.

[33] M. Yoshio, H. Wang, K. Fukuda, Y. Hara, Y. Adachi, Effect of carbon coating on electrochemical performance of treated natural graphite as lithium-ion battery anode material, J Electrochem Soc. 147 (2000) 1245–1250.

[34] N. Dimov, S. Kugino, M. Yoshio, Carbon-coated silicon as anode material for lithium ion batteries: Advantages and limitations, Electrochim. Acta 48 (2003) 1579–1587.

[35] R. Janus, P. Natkanski, A. Wach, M. Drozdek, Z. Piwowarska, P. Cool, P. Kustrowski, Thermal transformation of polyacrylonitrile deposited on SBA-15 type silica: Effect on adsorption capacity of methyl–ethyl ketone vapor, J. Therm. Anal. Calorim. 110 (2012) 119–125.

[36] M.S.A. Rahaman, A.F. Ismail, A. Mustafa, A review of heat treatment on polyacrylonitrile fiber, Polym. Degrad. Stab. 92 (2007) 1421–1432.

[37] D.M. Piper, T.A. Yersak, S.B. Son, S.C. Kim, C.S. Kang, K.H. Oh, C. Ban, A.C. Dillon, S.H. Lee, Conformal coatings of cyclized-PAN for mechanically resilient Si nano-composite anodes, Adv. Energy Mater. 3 (2013) 697–702.

[38] Y. Ma, L. Li, J. Qian, W. Qu, R. Luo, F. Wu, R. Chen, Materials and structure engineering by magnetron sputtering for advanced lithium batteries, Energy Storage Mater. 39 (2021) 203–224.

[39] K. Takada, N. Aotani, K. Iwamoto, S. Kondo, Solid state lithium battery with oxysulfide glass, Solid State Ionics 86-88 (1996) 877-882.

[40] J.M. Whiteley, J.W. Kim, C.S. Kang, J.S. Cho, K.H. Oh, S.H. Lee, Tin networked electrode providing enhanced volumetric capacity and pressureless operation for all-solid-state Li-ion batteries, J. Electrochem. Soc. 162 (2015) A711–A715.

[41] N.A. Dunlap, J.B. Kim, H. Guthery, C.-S. Jiang, I. Morrissey, C.R. Stoldt, K.H. Oh, M. Al-Jassim S.-H. Lee, Towards the commercialization of the all-solid-state Li-ion battery: Local bonding structure and the reversibility of sheet-style Si-PAN anodes, J. Electrochem. Soc. 167 (2020) 060522.

[42] S. Wenzel, T. Leichtweiss, D. Krüger, J. Sann, J. Janek, Interphase formation on lithium solid electrolytes—An in situ approach to study interfacial reactions by photoelectron spectroscopy, Solid State Ion. 278 (2015) 98–105.

[43] Y. He, X. Yu, Y. Wang, H. Li, X. Huang, Alumina-coated patterned amorphous silicon as the anode for a lithium-ion battery with high coulombic efficiency, Adv. Mater. 23 (2011) 4938–4941.

[44] X. Xiao, P. Lu, D. Ahn, Ultrathin multifunctional oxide coatings for lithium ion batteries, Adv. Mater. 23 (2011) 3911–3915.

[45] H. Zhu, M.H.A. Shiraz, L. Liu, Y. Hu, J. Liu, A facile and low-cost $Al_2O_3$ coating as an artificial solid electrolyte interphase layer on graphite/silicon composites for lithium-ion batteries, Nanotechnology 32 (2021) 144001.

# Chapter 3. Artificial Lithium phosphorus oxynitride Coating : Further Study.

## 3.1. Introduction

The development of industrialization has contributed to the progression of global warming. Consequently, interest in nonpolluting and eco-friendly energies is increasing. In particular, a battery, a device that stores energy, is significant for energy use, especially in the development of the automobile industry. However, the widely used Li-ion batteries have raised safety issues. All-solid-state batteries that use solid electrolytes have gained popularity as next-generation batteries because of their safety and high-capacity. Numerous energy and automotive experts predicted that EVs would replace internal combustion engines and become the mainstream of transportation. However, an electric vehicle must realize a mileage comparable to that of a traditional engine to replace it. Therefore, all-solid-state batteries should be developed with stability and high-capacity characteristics. A sulfide-based electrolyte, which is an all-solid electrolyte, exhibits excellent ionic conductivity but a low stability voltage window. The interfacial coating prevents electrolyte degradation and forms a stable SEI layer. Artificial SEI is one of the representative protective coatings [1-12].

Interfacial coatings should include the following features: 1) wide stability window voltage, 2) excellent Li-ion conductivity, and 3) low electronic

conductivity. Besides $Al_2O_3$, LiPON is a representative artificial coating material [13-18].

## 3.2. Artificial lithium phosphorus oxynitride coating

Among the various coating materials, artificial LiPON has a wide electrochemical voltage window (0.68 – 2.63 V vs $Li^+/Li$), reasonable ionic conductivity ($\sim 10^{-6}$ $S \cdot cm^{-1}$), and high electronic resistivity ($>10^{14}$ ohm·cm). The LiPON coating layer not only offers a pathway for Li-ion transport but also acts as a physical barrier preventing side reactions between the anode and the electrolyte. The improvements in capacity retention accomplished by the LiPON coating were attributed to a decrease in the electrolyte reduction reaction and the loss of lithium related to stable SEI formation. Notably, the thicker the $Al_2O_3$ coating, the lower the Li ion conductivity. However, as LiPON possesses Li-ion conductivity, it effectively limits electron transport by thick LiPON coating. In addition, thick coatings have the advantage of improving physical contact with the electrolyte [13-18].

## 3.3. Radio-frequency magnetron sputtering procedure

LiPON layers are deposited on Si-based anode by RF magnetron sputtering (25–50 W) of a $Li_3PO_4$ target (99.9% purity, Kurt J. Lesker) in a reactive $N_2$ atmosphere. The Si-based anode is placed on a glass holder, and the target-to-substrate distance is fixed as 5.0 cm. Before sputtering, argon gas is fed into the chamber (20 SCCM) and the target is presputtered to remove impurities on the target surface for 10 min. Argon and nitrogen gas flows are adjusted into the chamber. The thickness of the artificial LiPON coating is varied by changing the power (25–50 W), nitrogen ratio, and deposition time, resulting in a nanometer-scale coating on the anode [18].

## 3.4. Previous research

A stable interface between the anode (cathode) and the electrolyte is crucial for improving electrochemical performance. A stable SEI inhibits SEI growth and reduces the limited Li+ consumption. Therefore, electrolyte decomposition and interfacial resistance at the interface can be reduced through the artificial coating on the anode or cathode. As an effective strategy to overcome the interface issue, Shrestha et al. reported that an amorphous LiPON layer was deposited on NMC811 particles by RF magnetron sputtering. The LiPON-coated NMC811showed much lower charge transfer resistance after 20 cycles. Electrochemical impedance spectroscopy (EIS) results indicate that the LiPON layer forms a stable interface and improves long-term cycling characteristics [18].

## 3.5. Conclusion

The Si alloy-PAN anode is prepared with an artificial SEI layer using RF plasma. The interface is coated to prevent the decomposition of the sulfide-based electrolyte. There are various artificial interface coating materials, among which cycle performance was improved through the $Al_2O_3$ coating layer, as presented in this study. In addition, according to previous studies, LiPON coating can act as a passivating layer. The interfacial coating with a thickness of tens of nanometers widens the stability voltage window of the sulfide-based electrolyte and improves Li-ion movement into the anode. Moreover, it hinders the movement of electrons into the electrolyte, slows down the decomposition of the sulfide-based electrolyte, lowers the interfacial resistance, and reduces Li-ion consumption. Consequently, the cycle life and rate performance characteristics are improved. Interfacial coating at the anode is essential in all-solid-state batteries unless a solid electrolyte with a higher Li ion conductivity and a wider stability voltage window than sulfide-based electrolytes is developed. The electrochemical property of coating is improved in all-solid-state lithium-ion batteries. An appropriate artificial coating effectively prohibits Li-ion consumption and the growth of SEI layers during charging and discharging reactions.

## 3.6. References

[1] F. Wu, J. Maier, Y. Yu, Guidelines and trends for next-generation rechargeable lithium and lithium-ion batteries, Chem. Soc. Rev. 49, 1569 (2020).

[2] L. Xu, S. Tang, Y. Cheng, K. Wang, J. Liang, C. Liu, Y.- C. Cao, F. Wei, L. Mai, Interfaces in Solid-State Lithium Batteries, Joule, 2, (2018) 1991–2015.

[3] J. Lau, R.H. Deblock, D.M. Butts, D.S. Ashby, C.S. Choi, B.S. Dunn, Sulfide Solid Electrolytes for Lithium Battery Applications, Adv. Energy Mater. 8 1800933 (2018).

[4] Z. Wu, Z. Xie, A. Yoshida, Z. Wang, X. Hao, A. Abudula, G. Guan, Utmost Limits of Various Solid Electrolytes in All-Solid-State Lithium Batteries: A Critical Review, Renewable Sustain. Energy Rev. 109, (2019) 367–385.

[5] M. Du, K. Liao, Q. Lu, and Z. Shao, Recent advances in the Interface Engineering of Solid-State Li-ion Batteries with Artificial Buffer Layers: Challenges, Materials, Construction, and Characterization, Energy Environ. Sci. 12, (2019) 1780–1804.

[6] F. Zheng, M. Kotobuki, S. Song, M.O. Lai, L. Lu, Review on solid electrolytes for all-solid-state lithium- ion batteries, J. Power Sources 389 (2018) 198–213.

[7] Q. Wang, L. Jiang, Y. Yu, J. Sun, Progress of Enhancing the Safety of Lithium Ion Battery from the Electrolyte Aspect, Nano Energy 55, (2019) 93–114.

[8] M. Li, C. Wang, Z. Chen, K. Xu, J. Lu, New Concepts in Electrolytes, Chem. Rev. 120 (2020) 6783–6819.

[9] C. Wang, J. Liang, Y. Zhao, M. Zheng, X. Li, X. Sun, All-solid-state lithium batteries enabled by sulfide electrolytes: from fundamental research to practical engineering design, Energy Environ. Sci. 14 (2021) 2577–2619.

[10] C. Sun, J. Liu, Y. Gong, D.P. Wilkinson, J. Zhang, Recent advances in all-solid-state rechargeable lithium batteries, Nano Energy 33 (2017) 363–386.

[11] Y.-K. Sun, Promising All-Solid-State Batteries for Future Electric Vehicles, ACS Energy Lett. 5 3221–3223 (2020).

[12] H. Shen, E. Yi, L. Cheng, M. Amores, G. Chen, S.W. Sofie, M.M. Doeff, Solid-State Electrolyte Considerations for Electric Vehicle Batteries, Sustainable Energy Fuels 3, (2019) 1647–1659.

[13] S. Yu, H. Park, D. J. Siegel, Thermodynamic Assessment of Coating Materials for Solid-State Li, Na, and K Batteries, ACS Appl. Mater. Interfaces 11, (2019) 36607–36615.

[14] Y. Zhao, K. Zheng, X. Su, Addressing Interfacial Issues in Liquid-Based and Solid-State Batteries by Atomic and Molecular Layer Deposition, Joule 2 (2018) 2583–2604.

[15] Y. Zhu, X. He, Y. Mo, Origin of Outstanding Stability in the Lithium Solid Electrolyte Materials: Insights from Thermodynamic Analyses Based on First- Principles Calculations, ACS Appl. Mater. Interfaces 7, (2015) 23685–23693

[16] Y. -W. Byeon, H. Kim, Review on Interface and Interphase Issues in Sulfide Solid-State Electrolytes for All-Solid-State Li-Metal Batteries, MDPI Electrochem. 2, (2021) 452–471.

[17] Y. Li, D. Zhang, X. Xu, Z. Wang, Z. Liu, J. Shen, J. Liu, M. Zhu, Interface engineering for composite cathodes in sulfide-based all-solid-state lithium batteries, Journal of Energy Chemistry 60 (2021) 32–60.

[18] S. Shrestha, J. B. Kim, J. J. Jeong, H. J. Lee, S. C. Kim, H. J. Hah, K. H. Oh, S. -H. Lee, Effect of Amorphous LiPON Coating on Electrochemical Performance of $LiNi_{0.8}Mn_{0.1}Co_{0.1}O_2$ (NMC811) in All Solid-State Batteries, Journal of The Electrochemical Society, 168 (2021) 060537.

# Abstract in Korean

리튬 이차전지 기술은 기존의 소형 모바일 IT 기기는 물론 최근 전기자동차 (electric vehicles; EVs) 및 에너지 저장 시스템 (energy storage system; ESS)용 중대형 장치에 활용 범위가 늘어나면서 시장의 규모가 큰 폭으로 증가하고 있습니다. 에너지 절약, 환경 규제 강화, 화석 에너지 고갈 등으로 인하여 미래 자동차 산업은 친환경 전기 자동차로 패러다임이 전환되고 있습니다. 이에 따라 이차 전지의 수요 및 성능과 안전성 대한 요구도 급증하고 있습니다. 고용량, 안전성, 장수명 이차 전지 개발과 상용화를 위한 기술 개발이 핵심 소재와 셀 제조 기술 개발과 함께 병행되고 있습니다. 현재 리튬 이차 전지의 유기 액체 전해질은 가연성, 누액, 온도 취약성 등 안정성 이슈가 있습니다. 최근에는 화재의 원인이 되는 유기 액체전해질을 사용하지 않는 전고체 리튬이온 전지가 각광받고 있습니다. 불연성을 갖는 고체전해질은 높은 열적 안정성을 제공하고 폭발의 위험을 방지 할 수 있습니다.

액체 전해질은 배터리 내부 안정성을 높이기 위해 양극과 음극의 직접적인 접촉을 막는 분리막이 필요하지만, 고체 전해질은 그 자체로 분리막 역할을 합니다. 또한 분리막이 필요없기 때문에, 에너지 밀도를 높이는 활물질을 첨가할 수 있어 고밀도 배터리 구현도 가능합니다. 그리고 온도 변화로 인한 부반응이나 외부 충격에 의한 누액 위험이 없습니다.

두 번째 장에서는 음극과 고체 전해질 사이의 인공 $Al_2O_3$ 코팅 효과에 대한 연구를 보여줍니다. 고용량, 안전, 장수명의 이차전지 개발 요구와 함께 전고체 전지에 대한 관심이 높아지고 있습니다. 고체 배터리의 사이클 성능은 이온 확산을 방해하는 전해질-음극 계면의 계면 현상에 의해 제한됩니다. 다기능 $Al_2O_3$ 코팅이 실리콘 기반 음극의 전고체 리튬 이온 배터리에 적용되었습니다. $Al_2O_3$ 코팅은 실리콘 기반 음극에 안정적인 인공 고체 전해질 계면(SEI)을 제공합니다. $Al_2O_3$ 층은 Li-Al-O를 통한 리튬 이온의 확산을 증가시킬 뿐만 아니라 본질적으로 낮은 전자 전도로 인해 음극과 전해질 사이의 전자의 이동을 제한합니다. 간단하고 경제적인 $Al_2O_3$ 코팅을 생성하기 위해 무선 주파수 스퍼터링이 사용되었습니다. 실리콘 기반 음극의 사이클 특성은 얇은 비정질 알루미늄 산화물 층(즉, $Al_2O_3$ 코팅)을 추가하여 향상되었습니다.

100회 충전-방전 사이클 후, $Al_2O_3$ 층이 있는 하프 셀은 502.08 mAh $g^{-1}$의 방전 용량과 58.86%의 용량 유지율을 제공했습니다. 또한, 100 사이클에서 $Al_2O_3$ 층이 없는 샘플은 278.48 mAh $g^{-1}$의 방전 용량과 34.34%의 용량 유지율을 가졌습니다. 따라서, $Al_2O_3$로 코팅된 Si 기반 음극은 전고체 하프셀에서 높은 성능을 보여줍니다.

세 번째 장에서는 실리콘 기반 음극에 또 다른 인공 LiPON 코팅을 제안합니다. 연구자들은 양극 혹은 음극 위에 다양한 보호 코팅을 증착했습니다. 대표적인 보호 코팅 중 하나는 인공 SEI입니다. LiPON은 $Al_2O_3$를 제외한 가장 유망한 인공 코팅입니다. 넓고 안정적인 전압 범위와 우수한 Li 이온 확산성 및 낮은 전자 전도도 특성을 가집니다. $Al_2O_3$와 달리 LiPON은 그 자체로 우수한 리튬 이온 전도체이므로 상대적으로 두꺼운 코팅이 가능하고 전자 이동을 제한하는 데 상당히 효과적입니다. 결국 LiPON은 계면 저항을 줄이고 장기 사이클에서 우수한 특성을 나타낼 것으로 예상됩니다.

**핵심어 :** 전고체 전지, $Al_2O_3$ 계면 코팅, 안정적인 전압 범위, 실리콘 합금, PAN 코팅, RF 마그네트론 스퍼터링, LiPON 계면 코팅

**학번:** 2014-21440